Published in final edited form as:
Nat Commun. ; 5: 3827. doi:10.1038/ncomms4827.

Direct Observation of the Three Regions in α-Synuclein that Determine its Membrane-Bound Behaviour

Giuliana Fusco[1], **Alfonso De Simone**[2,*], **Gopinath Tata**[3], **Vitaly Vostrikov**[3], **Michele Vendruscolo**[1], **Christopher M. Dobson**[1,*], and **Gianluigi Veglia**[3,*]

[1]Department of Chemistry, University of Cambridge, Lensfield road, Cambridge UK, CB2 1EW

[2]Department of Life Sciences, Imperial College London, South Kensington, London UK, SW7 2AZ

[3]Department of Chemistry & Department of Biochemistry, Molecular Biology & Biophysics, University of Minnesota, 6-155 Jackson Hall 321 Church st. SE, Minneapolis USA, MN 55455

Abstract

α-synuclein (αS) is a protein involved in neurotransmitter release in presynaptic terminals, and whose aberrant aggregation is associated with Parkinson's disease. In dopaminergic neurons, αS exists in a tightly regulated equilibrium between water-soluble and membrane-associated forms. Here we used a combination of solid-state and solution-state NMR spectroscopy to characterize the conformations of αS bound to lipid membranes mimicking the composition and physical properties of synaptic vesicles. The study evidences three αS regions possessing distinct structural and dynamical properties, including an N-terminal helical segment having a role of membrane-anchor, an unstructured C-terminal region that is weakly associated with the membrane, and a central region acting as a sensor of the lipid properties and determining the affinity of αS membrane binding. Taken together, our data define the nature of the interactions of αS with biological membranes and provide insights into their roles in the function and in the molecular processes leading the aggregation of this protein.

Introduction

In the synaptic termini, the 140-residue protein α-synuclein (αS) is partitioned between cytosolic and membrane-associated forms[1]. Although the binding of αS to lipid membranes appears to be implicated in its functional role in synaptic regulation, it may also trigger its aggregation, ultimately leading to the formation of Lewy bodies, which are ubiquitously associated with Parkinson's disease, one of the most common types of neurodegenerative disorder[2-8].

*Correspondence and requests for materials should be addressed to vegli001@umn.edu, cmd44@cam.ac.uk and adesimon@imperial.ac.uk.

Authors Contribution

G.V., A.D., C.M.D., G.F., M.V., designed the experiments. G.F., A.D., V.V., G.T., performed the experiments. A.D., G.F., G.V., C.M.D. analysed the data. C.M.D., A.D., G.V., M.V., G.F. wrote the manuscript.

The authors declare no competing financial interests.

Europe PMC Funders Author Manuscripts

Understanding the structure and dynamics of the membrane-bound state of αS is therefore a major priority to clarify how for this protein the balance between functional and dysfunctional processes can be regulated. The dynamic nature of αS in both its cytosolic and membrane-bound states has, however, limited the application of standard methods of structural biology, including X-ray crystallography and solution-state NMR spectroscopy.

In its cytosolic form, αS can be monomeric and intrinsically disordered[9-11] or associated with other proteins[12]. Upon binding to lipid membranes, αS undergoes a significant conformational transition with respect to its monomeric intrinsically disordered form, with some regions adopting a high level of α-helical structure[13-16]. This ordering process is driven by specific amino acid patterns in the αS sequence, in particular those coding for amphipathic class A2 lipid-binding α-helical segments in the region of the molecule spanning residues from 1 to 90[16]. The modular organization of such α-helical fragments promotes αS binding to a wide variety of lipid assemblies, from micelles and lipid vesicles to cellular membranes[14, 15, 17, 18]. As a consequence of its metamorphic character, αS is able to sense membrane curvature and defects, and respond to the presence of specific features such as lipid rafts, adopting a range of structural architectures, such as a pair of anti-parallel curved α-helices (residues 3-37 and 45-92)[15, 17] or a single curved α-helix, encompassing essentially the entire N-terminal region[18-20]. Indeed, NMR studies involving lipids that mimic key features of synaptic vesicles, such as composition and curvature, have revealed that αS binds to lipid bilayers via a multiplicity of distinct binding modes[14].

Taken together these studies are providing a general view about the structural plasticity and the dynamical nature[21-23] of the membrane-bound state of αS, whose structural properties can sometimes be perturbed even by relatively minor external factors. It is therefore of fundamental importance to study the interactions of αS with lipids under conditions that reproduce as closely as possible the physical properties of presynaptic membranes. Small unilamellar vesicles (SUVs) with appropriate lipid mixtures of DOPE, DOPC and DOPS lipids have been shown to be excellent models for synaptic vesicles, but their slow tumbling rates prevent the detection of most of the signals from bound αS signals conventional solution-state NMR methods[14]. Under these experimental conditions, only resonances from the disordered C-terminus, the region of the protein having low membrane affinity, can be detected, while the segment of the protein containing residues that can interact strongly with membranes is essentially undetectable for solution-state NMR.

In this Communication, we show that it is possible to describe the conformational properties of the elusive membrane-bound state of αS by using a combination of solid-state NMR (ssNMR) spectroscopy and chemical exchange saturation transfer (CEST) measurements in solution NMR[24-26]. This approach proved to be highly effective in enabling the fine tuning between structural order and disorder in the membrane-bound state of αS to be probed directly without requiring any chemical modification of the protein or changes to its amino acid sequence.

We find from these studies that αS binds to the membranes of synaptic-like vesicles in such a manner that generates three different dynamical regimes in distinct regions of the protein sequence. Our combined approach indicates that αS interacts with synaptic-like vesicles via

an α-helical N-terminal 'anchor' which also enhances cooperatively the binding of the central region of the sequence to the membrane surface, while the C-terminal region remains largely unstructured and coupled only weakly to the cellular membrane. The central region includes also the 'non amyloid-β component' (NAC) fragment, that has been implicated in the mechanism of αS aggregation, and is here shown to play a key role in modulating the affinity of αS for cellular membranes. We therefore identify an essential region of the amino acid sequence of αS having a role in determining the way the protein partitions between membrane-bound and unbound states as well as in the processes of αS aggregation under pathological conditions leading to Parkinson's disease.

Results

Membrane bound αS features three distinct regions

We used ssNMR to probe the structural properties of αS bound to SUVs that mimic the native composition and curvature of synaptic vesicles[14]. The SUVs utilized in this study are acidic and consist of mixtures of 1,2-dioleoyl-sn-glycero-3- phosphoethanolamine (DOPE), 1,2-dioleoyl-sn-glycero-3-phospho-ʟ-serine (DOPS), and 1,2-dioleoyl-sn-glycero-3-phosphocholine (DOPC) in 5:3:2 molar ratios[14]. To characterize the conformational preferences of the αS bound state to these vesicles, we used a series of magic angle spinning (MAS) ssNMR techniques in conjunction with isotope labeling of the protein, an approach that has been shown to be a powerful means of studying interactions between proteins and membranes[27-32].

A solution of ^{13}C-^{15}N labeled αS was mixed with DOPE:DOPS:DOPC SUVs, as described previously[14] and in Methods. The resulting vesicles incorporating the labeled αS were subsequently packed into a 3.2 mm MAS rotor (Methods). Using circular dichroism, we selected a protein:lipid ratio of 1:65 by monitoring the transition of the protein signal from the disordered state to one with a high degree of α-helical structure, consequent upon addition of lipids (Supplementary Figure 1). With this protein-lipid ratio, the first 97 residues of αS are effectively invisible for solution NMR techniques because the association of αS with the SUVs broadens dramatically the protein resonances as a result of the slow tumbling of the complex in the absence of a very high degree of internal dynamics, such as that observed in the C-terminal region[14].

To investigate this elusive state we carried out a series of ssNMR experiments involving ^{13}C-^{13}C dipolar assisted rotational resonance (DARR)[33]. These spectra correlate both main-chain and side-chain ^{13}C labeled resonances of the protein, as a result of cross-polarization (CP) effects, and hence are able to detect rigid moieties of biomacromolecules even in the absence of rapid overall tumbling of the molecule. Indeed, in the study of interactions between proteins and membranes, DARR experiments have been shown to be particularly effective for detecting the resonances of residues that become highly rigid upon interaction with the lipid bilayer, such as for example transmembrane α-helices[30, 34]. Using a DARR contact time of 20 ms, we were able to detect homonuclear correlations between directly bonded carbon atoms in regions that are tightly bound to the membrane (Figure 1a,b). The highest signal intensities in the spectra of the samples studied here were obtained by performing the measurements at −19 °C, i.e. under conditions where the lipids adopt a

gel phase[35]; other than having increased signal-to-noise ratios, however, these spectra are fully consisting with those measured at 4 °C. Moreover, no variations in the number of observed resonances or the values of their chemical shifts were observed when the protein:lipid ratios were varied from 1:30 to 1:200.

DARR experiments performed at a range of different contact times (50, 100, 200 and 500 ms, Supplementary Figures 2 and 3) revealed an intense network of dipolar interactions, indicating that the ^{13}C-^{13}C DARR resonances belong to a well-defined structural segment of consecutive residues. The relatively low signal-to-noise ratios did not enable the acquisition of three-dimensional spectra, but we were nevertheless able to measure ^{15}N-^{13}C cross polarization correlations (Supplementary Figure 4) that have provided additional connectivities to those obtained from the ^{13}C-^{13}C DARR spectra.

The high redundancy in the αS primary sequence, which includes a series of conserved KTKEGV segments that are repeated imperfectly throughout the N-terminal region, poses a significant challenge for residue-specific assignments. Nonetheless, we were able to assign individual spin systems using ^{13}C-^{13}C DARR spectra recorded at different contact times, in conjunction with heteronuclear correlation experiments (Supplementary Figure 4) and information from the analysis of the chemical exchange saturation transfer (CEST) experiments (see below). As a consistency check, the chemical shifts of the assigned resonances were compared to those obtained by solution NMR experiments of αS in SDS and SLAS micelles[17, 36]. Overall, we have been able to obtain the sequential assignments for the segment K_6GLSKAKEGVVAAAEKTKQG_{25}. The ability to observe and assign the resonances of this stretch of the sequence revealed that the N-terminal segment of αS was sufficiently strongly anchored to the membrane to be visible using CP experiments. The measured chemical shifts values indicate that this αS segment was in a continuous α-helical conformation when bound to SUVs and, using the δ2D method[37], we estimated that the population of α-helical structure in this segment was on average 86 ± 11 % (Supplementary Figure 5).

In order to probe the effects of lipid composition on the affinity of αS for membranes, we studied the interactions of αS with SUVs consisting of 1-hexadecanoyl-2-(9Z-octadecenoyl)-sn-glycero-3-phospho-(1′-rac-glycerol) (POPG) lipids. αS has been shown to bind strongly to such lipid vesicles[38] and with an affinity that is approximately three fold higher than that found for DOPE:DOPS:DOPC SUVs[19]. This finding is in good agreement with our CD measurements which enabled apparent dissociation constants to be calculated and give values for K_d of 93 ± 15 μM for POPG and 261 ± 21 μM for DOPE:DOPS:DOPC SUVs under the conditions employed in the present study (Supplementary Figure 1). Despite the different binding affinities, however, no significant differences were observed between the DARR spectra of αS bound to POPG (Figure 2) and those of αS bound to DOPE:DOPS:DOPC vesicles (Figure 1a), indicating that the regions of the protein that are rigid in the membrane bound state are essentially identical for the two types of SUVs.

In addition to the DARR experiments, which provided direct evidence of the regions of αS that are tightly bound to the membranes, insensitive nuclei enhanced by polarization transfer (INEPT) MAS measurements[39] were used to monitor ^{1}H-^{13}C correlations of the most

dynamic parts of the protein in the bound state (Figure 1c). Such experiments have been shown to be highly effective probes of regions such as loops in cytoplasmic domains that possess extensive conformational fluctuations relative to those of the more rigid segments of membrane proteins. INEPT spectra of αS bound to DOPE:DOPS:DOPC SUVs showed a significant number of resonances that closely overlap with those observed in solution NMR ^{1}H-^{13}C HSQC spectra of αS in the presence of an excess of SUVs (Supplementary Figure 6). As the solution state ^{1}H-^{13}C HSQC spectra have been assigned[9, 14], the overlap of the spectra readily enabled the assignments of the MAS INEPT resonances to be defined (Figure 1c). The resulting assignments correspond to the region 97-140 and indicate that this fragment adopts unstructured conformations in the membrane-bound state. Overall the MAS measurements evidence three regions in the αS sequence, including a highly rigid N-terminal fragment adopting α-helical conformation, an unstructured C-terminal fragment and a central region, residues 26-96, that adopts an intermediate dynamical regime.

Probing the topology of αS bound to lipid bilayers

To probe the topology of the membrane bound state of αS, we employed paramagnetic relaxation enhancement (PREs) experiments[30]. For this purpose, we doped the DOPE:DOPS:DOPC SUVs with low levels (2%) of phospho-ethanolamine (PE) lipids that incorporate paramagnetic centres in the headgroups or at specific positions in the aliphatic chains[40]. In these experiments, the unpaired electrons from the paramagnetic centres increase the transverse relaxation rates of the nuclei in their vicinity, giving rise to line broadening and hence providing information on the proximity of individual residues of αS to different regions of the lipid bilayers.

As a paramagnetic probe, we first used the gadolinium salt of PE-DTPA (1,2-dimyristoyl-sn-glycero-3-phosphoethanolamine-N-diethylenetriaminepentaacetic acid, Avanti Polar Lipids Inc. Alabaster, USA), which carries an unpaired electron on the head group. We detected substantial paramagnetic broadening of a subset of resonances in the ^{13}C-^{13}C DARR spectrum of αS bound to SUVs doped with the probe molecule (Supplementary Figure 7a), and observed that hydrophilic residues are significantly more affected than hydrophobic ones. This pattern of behavior is typical of membrane-associated amphipathic sequences of proteins and peptides that form a α-helix that bound to the surface of the membrane, such that the hydrophilic residues are located at the water/headgroup interface and the hydrophobic residues are directed towards the inner core of the membrane (Supplementary Figure 7c). Interestingly, we also observed non-negligible attenuations of some of the signals in the ^{1}H-^{13}C INEPT spectrum of αS (Supplementary Figure 7b), including the positively charged K97, the uncharged polar residues Q99 and N103, and the hydrophobic residues L100, A107, I112 and V118. These findings indicate that the C-terminal region of αS interacts weakly and transiently with the membrane surface when bound to SUVs.

As these PRE measurements indicate that the N-terminal region of αS lies on the surface of lipid bilayer, to probe whether or not any part of αS inserts into the interior of the membrane, we used a second paramagnetic agent, 16-doxyl-PC (1-palmitoyl-2-stearoyl-[16-doxyl]-*sn*-glycero-3-phosphocholine, Avanti Polar Lipids Inc., USA). This molecule is

engineered with a paramagnetic doxyl group at position 16 of the hydrocarbon chain tail, which partitions within the lipid bilayer. We observed no significant paramagnetic relaxation effects on any of the αS resonances bound to SUVs, either in ^{13}C-^{13}C DARR or in ^{1}H-^{13}C INEPT spectra in the presence of this probe (Supplementary Figure 8). These MAS measurements rule out the possibility that any significant part of αS inserts even transiently into the membrane bilayer.

The central region of αS modulates membrane affinity

We next carried out a series of chemical exchange saturation transfer (CEST) experiments[24-26] to gain a deeper understanding of the equilibrium between the unbound and bound states of αS. The CEST approach is an ideal method for probing equilibria between NMR visible (detectable) and invisible (undetectable) states of proteins, including low molecular weight species that are transiently bound to slow-tumbling high-molecular-weight complexes, which indeed cannot be observed directly in solution NMR experiments as a result of excessive line broadening. In the CEST experiments, a continuous weak radiofrequency field is applied off-resonance (by up to 28 kHz) in the ^{15}N channel, thereby saturating the broad spectroscopic transitions in the bound (undetectable) state but leaving the resonances of the free (detectable) state virtually unperturbed[24-26]. The saturation of the bound state can then be transferred to the free state *via* chemical exchange, attenuating the intensities of the observable resonances of the latter. By carrying out a series of experiments at various offsets, it is possible to obtain a map of the strength of interactions between the low and high molecular weight species at a residue specific resolution.

In the presence of a small quantity of SUVs (0.06% of lipid mixture, 0.6 mg ml^{-1}) all of the αS resonances are detectable in the ^{1}H-^{15}N HSQC spectra, and only marginal changes in the peak intensities are observed. By contrast, substantial differences are observed in CEST experiments (Figure 3a and Supplementary Figure 10), which in the presence of SUVs evidenced specific resonances from the protein sequence that exhibit strong saturation effects over a broad range of offsets resulting in symmetric CEST profiles (Figure 3b). In probing the interactions between αS and DOPC:DOPE:DOPS SUVs, these experiments show clearly that the strongest saturation effects are observed for residues in the N-terminal region of the protein, indicating that this segment has a tighter association with the SUVs than any other region of the protein (Figure 3b). The saturation effects decrease gradually for residues 26-97 with a sharp transition in the vicinity of residue 98, where the peak intensities of the resonances coincide with those observed in the absence of lipids (Supplementary Figure 9). These experiments therefore provide a residue-specific measure of the magnitude of the interactions between αS and DOPC:DOPE:DOPS SUVs, and these results are fully consistent with the conclusions of the ssNMR experiments discussed above. Together these findings reveal that the N-terminal region of αS bound to SUVs forms a stable helix that interacts strongly with the surface of the lipid bilayer while the C-terminal region of the protein is highly dynamic and motionally independent of the SUVs.

The CEST experiments were repeated with SUVs prepared with POPG lipids[38] (Figures 3c and Supplementary Figure 11). The saturation profiles obtained under these conditions are generally similar to those obtained with DOPC:DOPE:DOPS SUVs, where resonances of

residues of the membrane-associated N-terminus are strongly affected by off-resonance saturation, while those of the residues of the C-terminus are essentially unchanged in intensity. A significant difference in the saturation profiles is, however, found for the central region of the sequence (residues 26-97) which shows remarkably stronger levels of saturation when bound to SUVs composed of POPG lipids (Figure 3c) compared to those observed in the presence of DOPE:DOPC:DOPS SUVs (Figure 3a,b). These data suggest that different regions of αS have distinct roles in the process of association with lipid membranes, such that the N-terminal α-helix (residues 6-25) acts to anchor αS strongly to the membrane, and is only marginally affected by lipid composition, while the region 26-97 appear to act as a membrane 'sensor', modulating the strength of the interactions in a lipid-specific manner (Figure 4).

Discussion

Although it is now generally recognized that the formation of fibrillar aggregates by αS is a hallmark of Parkinson's disease, much remains to be understood about the physiological role of this protein[6]. αS possesses an eclectic character and the ability to adopt different conformations resulting in a variety of cytosolic, membrane-bound and aggregated states. In aqueous solutions[9] as well as in cellular milieu[10], αS has been shown to behave as an intrinsically disordered protein, although there has been evidence for and against the possible existence of more highly structured forms of soluble αS in some environments and in complexes[41, 42]. Considerable attention has also been focused on the membrane-associated state of αS, which has been suggested to be of great significance in both physiological and pathological contexts. It is indeed evident that αS exists *in vivo* in an equilibrium between cytosolic and membrane-bound states, with membrane partitioning being tightly regulated[1, 12].

A particularly intriguing issue in this context is the mechanism by which the affinity of αS to lipid membranes is modulated. There is strong evidence that the population of the bound state is regulated by the intrinsic structural properties of αS and on the composition and the physical properties of the membrane bilayer, such as curvature, charge, packing defects and surface hydrophobicity[15, 17, 18, 36, 43].

We explored this fundamental issue by probing the structure and conformational dynamics of αS bound to membranes in its physiological, non-aggregated state. This membrane-bound state is effectively intractable to current X-ray crystallography techniques but the success of solution state NMR spectroscopy in describing the disordered soluble protein [9, 10, 13-17, 36, 44, 45] and of solid state NMR studies in defining the structural properties of the polymorphic forms of the aggregated state of αS[46-49] has prompted us to explore the use of a combination of these techniques to define the structures and dynamics of αS bound in its non-aggregated state to lipid membranes.

Our approach could directly probe the interaction with lipid mixtures that mimic those of synaptic vesicles without requiring alterations of the protein sequence or any chemical modification. We have found that, in line with the metamorphic nature of αS[50], three distinct regions of this protein (the N-terminal, central, and C-terminal segments) interact in

very different ways with lipid bilayers as a result of their different structural and dynamical properties (Figure 4). The N-terminal 25 residues, which we denote as the membrane anchor region, adopt a well-defined and highly motionally restricted α-helical conformation that appears to be largely independent of lipid composition. By contrast, the central segment of the protein (residues 26-97), which can be described as a membrane-sensor region, has intermediate dynamical properties. This region is indeed too flexible to be detected by cross-polarization experiments but too rigid to be seen by INEPT-type transfer experiments. It is legitimate to assume, based on EPR measurements[18, 20] and transferred NOE data[14], that this membrane-sensor region adopts α-helical structure when transiently bound to a lipid membrane surface. The present results indicate that the NAC sequence, which has been shown to play a role in the mechanisms of αS aggregation[6, 51-53], being included in the membrane-sensor region is also likely to have functional relevance, specifically in defining the affinity of αS for lipid membranes and therefore to modulate the partitioning between membrane-bound and membrane-free states in the synaptic termini. Finally, we have found from PRE experiments that the C-terminal domain (residues 99-140), which has been reported to be highly unstructured and extremely flexible, experiences weak and transient interactions with the membrane surface.

In conclusion, by combining solution and solid-state NMR techniques, we have characterised a series of key structural features of the membrane-bound state of αS, and to define the nature of its interactions with lipid assemblies (SUVs) that mimic synaptic-like lipid membranes. From these data, emerged a model to describe the interactions of αS with membranes, which reconciles the results of a range of previous studies[13-20, 36] and also sheds new light on the molecular determinants of binding affinity that are likely to be associated with the physiological role of αS. The membrane interactions in the processes of αS aggregation underscores the importance of the interplay between different functional states of αS and its aggregation mechanism leading to Parkinson's disease.

Methods

αS purification

αS was purified in E. coli using plasmid pT7-7 encoding for the protein as previously described[54]. See Supplementary Methods for further details.

Preparation of SUVs for solid state and solution NMR

Small unilamellar vesicles (SUVs) containing a molar ratio of 5:3:2 of DOPE:DOPS:DOPC (Avanti Polar Lipids Inc., USA) were prepared from chloroform solution of the lipid. The lipid mixture was evaporated under a stream nitrogen gas and then dried thoroughly under vacuum, to yield a thin lipid film. Then the dried thin film was re-hydrated adding an aqueous buffer (20 mM sodium phosphate, pH 6.0) and subjected to vortex mixing. Several cycles of freeze-thawing cycles and sonication were carried out until the mixture become clear. In the case of CEST experiments, after sonication, SUVs were mixed with αS samples with a concentration of 0.06% (0.6 mg ml^{-1}). In the case of ssNMR, after sonication, αS was then added to the SUVs mixture up to a molar ratio of 1:65 protein:lipid. Then the mixture was pelleted at 75k (13,500 rpm) for 30 min and 4°C (Beckman Coulter Optima

TLX Inc. Brea, USA) by using a rotor TLA 100.3. Subsequently the SUV-αS sample was transferred to 3.2 mm Zirconia XC thin-walled MAS rotor for the SSNMR experiments. POPG SUV-αS samples were prepared using the same protocol but a 50 mM potassium phosphate buffer and 100 mM NaCl at pH 7.4 was used.[19]

Magic angle spinning measurements

All MAS experiments were carried out on either a 14.09T or a 16.85T VNMRS Spectrometer with a 3.2 mm BioMASTM probe (Agilent Technologies, USA). Dipolar assisted rotational resonance (DARR) experiments[33] were performed on a MAS rate of 10 kHz using different contact time (20, 50, 100, 200 and 500 ms). DARR were acquired at −19 °C and 4 °C (the latter is for control experiments only). Insensitive nuclei enhanced by polarization transfer (INEPT) were carried out at 4 °C using a MAS rate of 10 kHz. Pulse widths were 2.5 μs for ^{1}H and 5.5 μs for ^{13}C and proton TPPM decoupling was applied at ωRF/(2π) = 71.4-100 kHz. DARR experiments were acquired using a 1 ms CP time and a DARR contact times ranging from 50ms to 500ms.

Solution NMR samples and CEST experiments

Solution NMR experiments were carried out at 10 °C on Bruker spectrometers operating at ^{1}H frequencies of 700 MHz equipped with triple resonance HCN cryo-probes. CEST experiments were based on ^{1}H-^{15}N HSQC experiments by applying constant wave saturation in the ^{15}N channel. As the exchange is probed between monomeric αS (having sharp resonances) and the slow tumbling SUVs-bound state (having significantly broad resonances), a series of large offsets was employed (−28, −21, −14, −9, −5, −3, −1.5, 0, 1.5, 3, 5, 9, 14, 21 and 28 kHz) resulting in CEST profiles of symmetric shape (Figure 3a). An additional spectrum, saturated at −100 kHz was recorded as reference. CEST experiments were performed using two continuous wave radio frequencies (170Hz and 350Hz) to saturate ^{1}H-^{15}N-HSQC spectra recorded using a data matrix consisting of 2048 (t_2, ^{1}H) × 440 (t_1, ^{15}N) complex points. Assignments of the spectra resonances in for ^{1}H-^{15}N-HSQC spectra in solution NMR were obtained from previous works of the lab[2, 9, 14].

Supplementary Material

Refer to Web version on PubMed Central for supplementary material.

Acknowledgments

We acknowledge financial support from Parkinson's UK (GF), Wellcome Trust (CMD, MV), Medical Research Council UK (CMD, MV), NIH (GV), Leverhulme Trust (AD). We thank Dr. Youlin Xia for technical assistance in solution NMR.

Abbreviations

αS	α-synuclein
CEST	chemical exchange saturation transfer
CP	cross polarization

DARR	dipolar assisted rotational resonance
DOPC	1,2-dioleoyl-sn-glycero-3-phosphocholine
DOPE	1,2-dioleoyl-sn-glycero-3- phosphoethanolamine
DOPS	1,2-dioleoyl-sn-glycero-3-phospho-L-serine
EPR	electron paramagnetic resonance
INEPT	insensitive nuclei enhanced by polarization transfer
NAC	non amyloid-β component
NOE	nuclear overhauser effect
NMR	nuclear magnetic resonance
ssNMR	solid state NMR
MAS	magic angle spinning
PE-DTPA	1,2-dimyristoyl-sn-glycero-3-phosphoethanolamine-N-diethylenetriaminepentaacetic acid
POPG	1-hexadecanoyl-2-(9Z-octadecenoyl)-sn-glycero-3-phospho-(1′-rac-glycerol)
PE	phospho-ethanolamine
PRE	paramagnetic relaxation enhancement
SUVs	small unilamellar vesicles

References

1. Lee HJ, Choi C, Lee SJ. Membrane-bound alpha-synuclein has a high aggregation propensity and the ability to seed the aggregation of the cytosolic form. J. Biol. Chem. 2002; 277:671–678. [PubMed: 11679584]
2. Bodner CR, Maltsev AS, Dobson CM, Bax A. Differential phospholipid binding of alpha-synuclein variants implicated in Parkinson's disease revealed by solution NMR spectroscopy. Biochemistry. 2010; 49:862–871. [PubMed: 20041693]
3. Perrin RJ, Woods WS, Clayton DF, George JM. Interaction of human alpha-Synuclein and Parkinson's disease variants with phospholipids. Structural analysis using site-directed mutagenesis. J Biol. Chem. 2000; 275:34393–34398. [PubMed: 10952980]
4. Comellas G, Lemkau LR, Zhou DH, George JM, Rienstra CM. Structural intermediates during alpha-synuclein fibrillogenesis on phospholipid vesicles. J. Am. Chem. Soc. 2012; 134:5090–5099. [PubMed: 22352310]
5. Breydo L, Wu JW, Uversky VN. Alpha-synuclein misfolding and Parkinson's disease. Bioch. Bioph. acta. 2012; 1822:261–285.
6. Chiti F, Dobson CM. Protein misfolding, functional amyloid, and human disease. Ann. Rev. Bioch. 2006; 75:333–366.
7. Dobson CM. Protein folding and misfolding. Nature. 2003; 426:884–890. [PubMed: 14685248]
8. Uversky VN, Li J, Fink AL. Evidence for a partially folded intermediate in alpha-synuclein fibril formation. J. Biol. Chem. 2001; 276:10737–10744. [PubMed: 11152691]
9. Dedmon MM, Lindorff-Larsen K, Christodoulou J, Vendruscolo M, Dobson CM. Mapping long-range interactions in alpha-synuclein using spin-label NMR and ensemble molecular dynamics simulations. J. Am. Chem. Soc. 2005; 127:476–477. [PubMed: 15643843]

10. Waudby CA, et al. In-cell NMR characterization of the secondary structure populations of a disordered conformation of alpha-synuclein within E. coli cells. PloS one. 2013; 8:e72286. [PubMed: 23991082]
11. Weinreb PH, Zhen W, Poon AW, Conway KA, Lansbury PT Jr. NACP, a protein implicated in Alzheimer's disease and learning, is natively unfolded. Biochemistry. 1996; 35:13709–13715. [PubMed: 8901511]
12. Uversky VN, Eliezer D. Biophysics of Parkinson's disease: structure and aggregation of alpha-synuclein. Curr. Prot. Pept. Sci. 2009; 10:483–499.
13. Maltsev AS, Ying J, Bax A. Impact of N-terminal acetylation of alpha-synuclein on its random coil and lipid binding properties. Biochemistry. 2012; 51:5004–5013. [PubMed: 22694188]
14. Bodner CR, Dobson CM, Bax A. Multiple tight phospholipid-binding modes of alpha-synuclein revealed by solution NMR spectroscopy. J. Mol. Biol. 2009; 390:775–790. [PubMed: 19481095]
15. Ulmer TS, Bax A. Comparison of structure and dynamics of micelle-bound human alpha-synuclein and Parkinson disease variants. J. Biol. Chem. 2005; 280:43179–43187. [PubMed: 16166095]
16. Eliezer D, Kutluay E, Bussell R Jr. Browne G. Conformational properties of alpha-synuclein in its free and lipid-associated states. J. Mol. Biol. 2001; 307:1061–1073. [PubMed: 11286556]
17. Ulmer TS, Bax A, Cole NB, Nussbaum RL. Structure and dynamics of micelle-bound human alpha-synuclein. J. Biol. Chem. 2005; 280:9595–9603. [PubMed: 15615727]
18. Jao CC, Hegde BG, Chen J, Haworth IS, Langen R. Structure of membrane-bound alpha-synuclein from site-directed spin labeling and computational refinement. Proc. Natl. Acad. Sci. USA. 2008; 105:19666–19671. [PubMed: 19066219]
19. Lokappa SB, Ulmer TS. Alpha-synuclein populates both elongated and broken helix states on small unilamellar vesicles. J. Biol. Chem. 2011; 286:21450–21457. [PubMed: 21524999]
20. Cheng CY, Varkey J, Ambroso MR, Langen R, Han S. Hydration dynamics as an intrinsic ruler for refining protein structure at lipid membrane interfaces. Proc. Natl. Acad. Sci. USA. 2013; 110:16838–16843. [PubMed: 24082088]
21. Fuxreiter M, Tompa P. Fuzzy complexes: a more stochastic view of protein function. Adv. Exp. Med. Bio. 2012; 725:1–14. [PubMed: 22399315]
22. Fuxreiter M. Fuzziness: linking regulation to protein dynamics. Mol. bioSystems. 2012; 8:168–177.
23. Tompa P, Fuxreiter M. Fuzzy complexes: polymorphism and structural disorder in protein-protein interactions. Trend Biochem. Sci. 2008; 33:2–8. [PubMed: 18054235]
24. Vallurupalli P, Bouvignies G, Kay LE. Studying "invisible" excited protein states in slow exchange with a major state conformation. J. Am. Chem. Soc. 2012; 134:8148–8161. [PubMed: 22554188]
25. Fawzi NL, Ying J, Ghirlando R, Torchia DA, Clore GM. Atomic-resolution dynamics on the surface of amyloid-beta protofibrils probed by solution NMR. Nature. 2011; 480:268–272. [PubMed: 22037310]
26. Milojevic J, Esposito V, Das R, Melacini G. Understanding the molecular basis for the inhibition of the Alzheimer's Abeta-peptide oligomerization by human serum albumin using saturation transfer difference and off-resonance relaxation NMR spectroscopy. J. Am. Chem. Soc. 2007; 129:4282–4290. [PubMed: 17367135]
27. Cady SD, Schmidt-Rohr K, Wang J, Soto CS, Degrado WF, Hong M. Structure of the amantadine binding site of influenza M2 proton channels in lipid bilayers. Nature. 2010; 463:689–692. [PubMed: 20130653]
28. Krepkiy D, et al. Structure and hydration of membranes embedded with voltage-sensing domains. Nature. 2009; 462:473–479. [PubMed: 19940918]
29. Wang S, et al. Solid-state NMR spectroscopy structure determination of a lipid-embedded heptahelical membrane protein. Nature methods. 2013; 10:1007–1012. [PubMed: 24013819]
30. Gustavsson M, et al. Allosteric regulation of SERCA by phosphorylation-mediated conformational shift of phospholamban. Proc. Natl. Acad. Sci. USA. 2013; 110:17338–17343. [PubMed: 24101520]
31. Lange A, et al. Toxin-induced conformational changes in a potassium channel revealed by solid-state NMR. Nature. 2006; 440:959–962. [PubMed: 16612389]

32. Grobner G, Burnett IJ, Glaubitz C, Choi G, Mason AJ, Watts A. Observations of light-induced structural changes of retinal within rhodopsin. Nature. 2000; 405:810–813. [PubMed: 10866205]
33. Takegoshi K, Terao T. 13C-1H dipolar recoupling under very fast magic-angle spinning using virtual pulses. Solid state nuclear magnetic resonance. 1999; 13:203–212. [PubMed: 10378429]
34. Traaseth NJ, Shi L, Verardi R, Mullen DG, Barany G, Veglia G. Structure and topology of monomeric phospholamban in lipid membranes determined by a hybrid solution and solid-state NMR approach. Proc. Natl. Acad. Sci. USA. 2009; 106:10165–10170. [PubMed: 19509339]
35. Nagle JF, Tristram-Nagle S. Structure of lipid bilayers. Bioc. Bioph. Acta. 2000; 1469:159–195.
36. Rao JN, Jao CC, Hegde BG, Langen R, Ulmer TS. A combinatorial NMR and EPR approach for evaluating the structural ensemble of partially folded proteins. J. Am. Chem. Soc. 2010; 132:8657–8668. [PubMed: 20524659]
37. Camilloni C, De Simone A, Vranken WF, Vendruscolo M. Determination of Secondary Structure Populations in Disordered States of Proteins Using Nuclear Magnetic Resonance Chemical Shifts. Biochemistry. 2012; 51:2224–2231. [PubMed: 22360139]
38. Li C, Lutz EA, Slade KM, Ruf RA, Wang GF, Pielak GJ. 19F NMR studies of alpha-synuclein conformation and fibrillation. Biochemistry. 2009; 48:8578–8584. [PubMed: 19655784]
39. Morris GA, Freeman R. Enhancement of nuclear magnetic-resonance signals by polarization transfer. J. Am. Chem. Soc. 1979; 101:760–762.
40. Al-Abdul-Wahid MS, Verardi R, Veglia G, Prosser RS. Topology and immersion depth of an integral membrane protein by paramagnetic rates from dissolved oxygen. J. Biomol. NMR. 2011; 51:173–183. [PubMed: 21947925]
41. Bartels T, Choi JG, Selkoe DJ. alpha-Synuclein occurs physiologically as a helically folded tetramer that resists aggregation. Nature. 2011; 477:107–110. [PubMed: 21841800]
42. Fauvet B, et al. alpha-Synuclein in central nervous system and from erythrocytes, mammalian cells, and Escherichia coli exists predominantly as disordered monomer. J. Biol. Chem. 2012; 287:15345–15364. [PubMed: 22315227]
43. Ouberai MM, et al. alpha-Synuclein senses lipid packing defects and induces lateral expansion of lipids leading to membrane remodeling. J. Biol. Chem. 2013; 288:20883–20895. [PubMed: 23740253]
44. Kang L, Wu KP, Vendruscolo M, Baum J. The A53T mutation is key in defining the differences in the aggregation kinetics of human and mouse alpha-synuclein. J. Am. Chem. Soc. 2011; 133:13465–13470. [PubMed: 21721555]
45. Leftin A, Job C, Beyer K, Brown MF. Solid-state (1)(3)C NMR reveals annealing of raft-like membranes containing cholesterol by the intrinsically disordered protein alpha-Synuclein. J. Mol. Biol. 2013; 425:2973–2987. [PubMed: 23583776]
46. Gath J, Bousset L, Habenstein B, Melki R, Meier BH, Bockmann A. Yet another polymorph of alpha-synuclein: solid-state sequential assignments. Biomol. NMR Ass. in press. 2013
47. Bousset L, et al. Structural and functional characterization of two alpha-synuclein strains. Nature communications. 2013; 4:2575.
48. Gath J, Habenstein B, Bousset L, Melki R, Meier BH, Bockmann A. Solid-state NMR sequential assignments of alpha-synuclein. Biomol. NMR Ass. 2012; 6:51–55.
49. Heise H, Hoyer W, Becker S, Andronesi OC, Riedel D, Baldus M. Molecular-level secondary structure, polymorphism, and dynamics of full-length alpha-synuclein fibrils studied by solid-state NMR. Proc. Natl. Acad. Sci. USA. 2005; 102:15871–15876. [PubMed: 16247008]
50. Uversky VN. A protein-chameleon: conformational plasticity of alpha-synuclein, a disordered protein involved in neurodegenerative disorders. J. Biom. Str. Dyn. 2003; 21:211–234.
51. Ueda K, et al. Molecular cloning of cDNA encoding an unrecognized component of amyloid in Alzheimer disease. Proc. Natl. Acad. Sci. USA. 1993; 90:11282–11286. [PubMed: 8248242]
52. Cookson MR. The biochemistry of Parkinson's disease. Ann. Rev. Biochem. 2005; 74:29–52. [PubMed: 15952880]
53. Karpinar DP, et al. Pre-fibrillar alpha-synuclein variants with impaired beta-structure increase neurotoxicity in Parkinson's disease models. EMBO J. 2009; 28:3256–3268. [PubMed: 19745811]

54. Hoyer W, Antony T, Cherny D, Heim G, Jovin TM, Subramaniam V. Dependence of alpha-synuclein aggregate morphology on solution conditions. J. Mol. Biol. 2002; 322:383–393. [PubMed: 12217698]

Europe PMC Funders Author Manuscripts

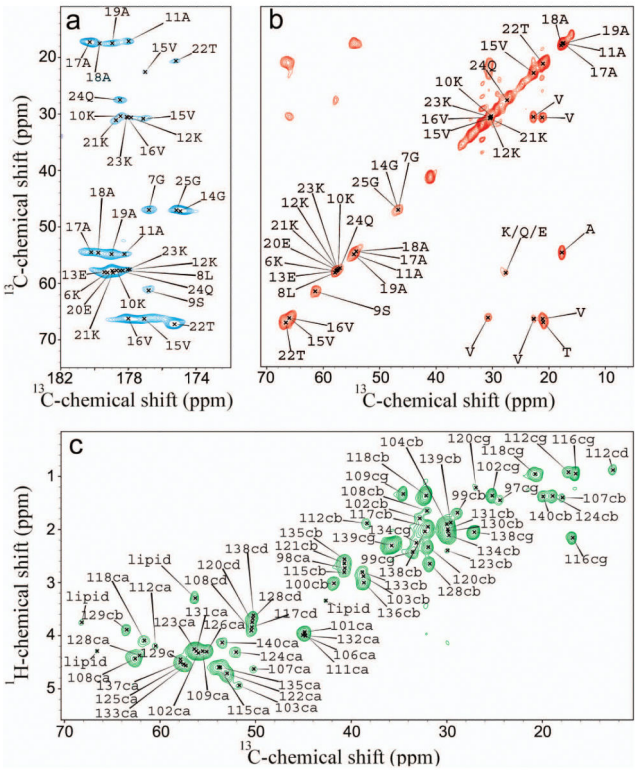

Figure 1. MAS ssNMR spectrum of αS bound to DOPE:DOPS:DOPC SUVs

^{13}C-^{13}C DARR correlation spectrum recorded at −19 °C using a 20 ms contact time at a MAS rate of 10 kHz. Carbonyl and aliphatic regions are showed in panels A and B, respectively. Residue names are reported using the single letter convention. **c)** ^{1}H-^{13}C correlation via INEPT transfer recorded at 4 °C at a MAS rate of 10 kHz. The experiments were performed at ^{1}H frequencies of 600 and 700 MHz using a ^{1}H/^{13}C 3.2-mm probe and a spinning speed of 10.0 kHz. Atom names ca, cb, cg, cd are used for C^{α}, C^{β}, C^{γ} and C^{δ} atoms, respectively.

Europe PMC Funders Author Manuscripts

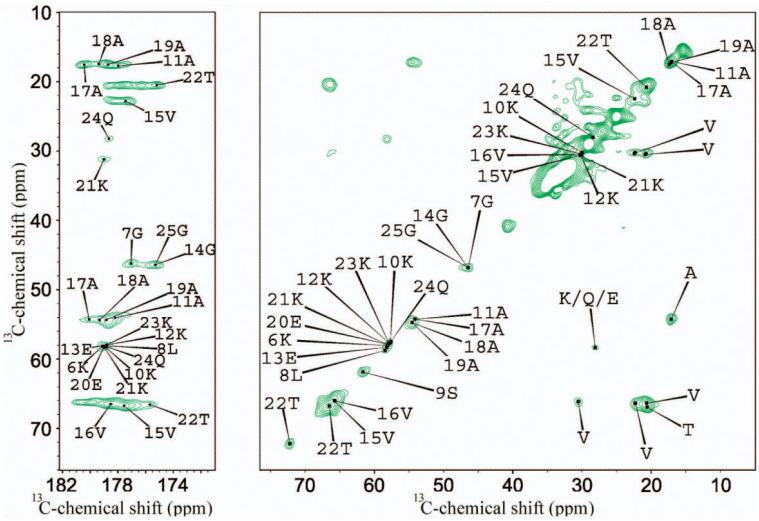

Figure 2. MAS ssNMR spectrum of αS bound to POPG SUV

The carbonyl region (left panel) and the aliphatic region (right panel) are shown in a ^{13}C-^{13}C DARR correlation spectrum of a sample of αS bound to POPG SUV recorded using a contact time of 100 ms at a temperature of −19 °C at a MAS rate of 10 kHz. Residue names are reported using the single letter convention.

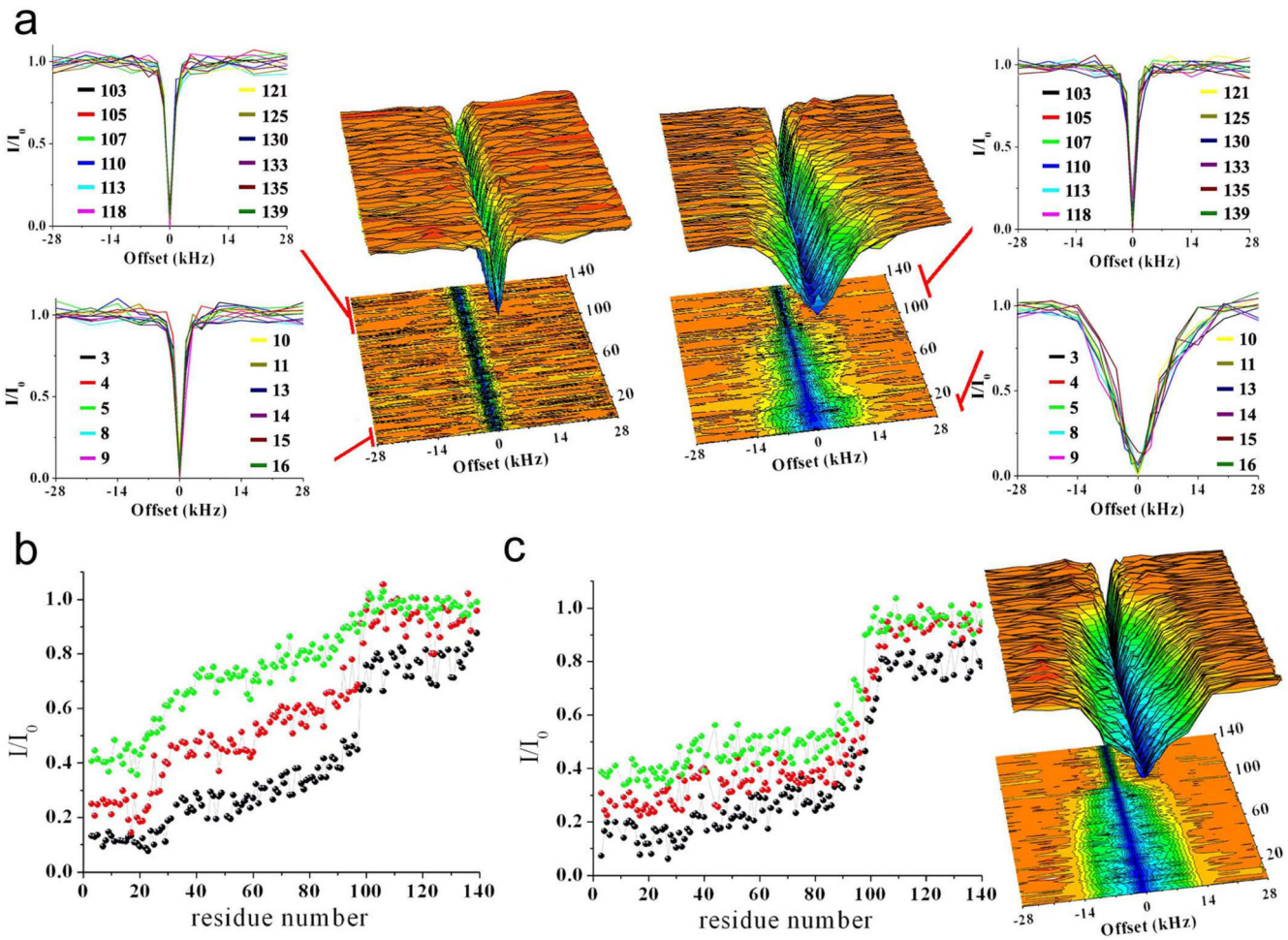

Figure 3. CEST experiments probing the membrane-sensor interactions of αS

CEST experiments were recorded at a ^{1}H frequency of 700 MHz (see Methods), using a protein concentration of 300 μM and 0.06% (0.6 mg ml^{-1}) of DOPE:DOPS:DOPC lipids in a ratio of 5:3:2 and assembled in SUVs. ^{1}H-^{15}N HSQC spectra were recorded by using a continuous wave saturation (170 Hz or 350 Hz) on the ^{15}N channel at a range of offsets: −28, −21, −14, −9, −5, −3, −1.5, 0, 1.5, 3, 5, 9, 14, 21 and 28 kHz. An additional spectrum, saturated at −100 kHz was recorded as a reference. Data recorded using 350 Hz are shown (data measured using 170 Hz are reported in Supplementary Figure 10). **a)** CEST surface for unbound (left) and bound (right) αS; the upper and lower inserts report individual CEST profiles for residues at the N- and C-termini, respectively. **b)** CEST saturation along the αS sequence. Black lines refer to the averaged CEST profiles measured using offsets at +/− 1.5 kHz. Similarly, profiles for +/− 3 kHz and +/− 5 kHz are shown in red and green, respectively. **c)** The interactions between αS and POPG SUVs probed by CEST. Labels as in panel b. The data were measured using 350 Hz, (see Supplementary Figure 11 for data acquired using 170 Hz).

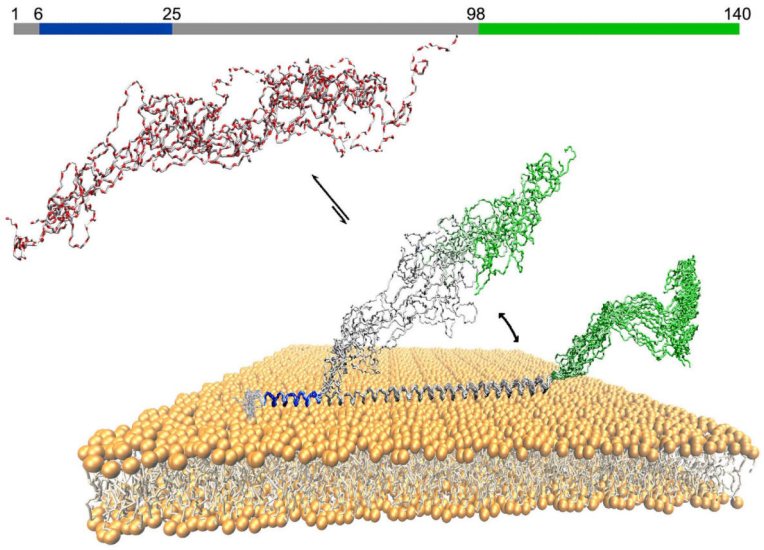

Figure 4. Schematic illustration of the different roles of the three regions in of αS in determining its interaction with lipid bilayers

We identified three different regimes of protein dynamics and membrane affinity by using a combination of solution and solid state NMR spectroscopy. The N-terminal region (blue) is visible in DARR experiments, indicating that it is rigidly bound and anchored to the membrane. The central region (grey), showing intermediate dynamics and therefore being invisible in both CP and INEPT experiments, is suggested to play a key role in modulating the affinity of αS for membranes. Finally a C-terminal fragment (green) maintains its unstructured nature and remains essentially uncorrelated with the membrane surface, despite showing weak and transient contacts in PRE experiments.